Paper presented at the Korean Rock Mechanics Society, Seoul in March 1995

Permanent Support for Tunnels using NMT

by Nick Barton NGI, Oslo Norway

ABSTRACT
Key aspects of the Norwegian Method of Tunnelling (NMT) are reviewed. These include a predictive method of support design using the six-parameter Q-system of rock mass characterisation. The rock mass rating or Q-value is updated during tunnel driving. The designed tunnel support generally consists of wet process, steel fibre reinforced shotcrete combined with fully grouted, untensioned rock bolts. Even in poor rock conditions S(fr) + B usually acts as the final rock reinforcement and tunnel lining. Since it is a drained lining, it is very economic compared to cast concrete with membranes. Light, free-standing steel liners are used to prevent water affecting the tunnel environment. Rock mass conditions, and hence lining design and cost estimation can be assessed by careful use of seismic surveys. Relationships between the P-wave velocity, the rock mass deformation modulus and the Q-value have recently been established, where tunnel depth, rock porosity and the uniaxial compression strength of the rock are important variables. The rock mass modulus estimate, and simple index testing of the joints, provide the key input data for numerical verification of the designs. Distinct element modelling in which joints are discretely represented (either in two dimensions with the UDEC code or in three dimensions with the 3DEC code) is generally favoured compared to continuum analysis. The latter may give a misleading impression of uniformity and deformations tend to be underestimated. Q-system NMT designs of S(fr) + B (fibre reinforced shotcrete and bolting) are numerically checked and adjustments made to bolt capacities and shotcrete thickness if overloading is evident around the modelled profile.

INTRODUCTION TO NMT

The extensive hydropower development in Norway in the 1960s and 1970s and major road tunnel developments in the 1980s and 1990s have maintained a tunnelling activity of some 100 km per year for much of the last 25 years. It is seldom that less than 3 million cubic metres of rock is excavated for tunnels or caverns in any one year. Norway has some 180 underground hydroelectric power plant more or less one half of the world's total built underground. Recently, we have surprised even ourselves with a 60 metre span sports hall in rock for the 1994 Winter Olympic Games. This is by far the largest cavern for public use (accommodating some 5,400 spectators) and was constructed in eight months in jointed gneiss that even the Japanese acknowledge to be well jointed, with seldom less than 2 to 4 joints per metre, and an average RQD of only 70%.

While many other countries automatically assume the extra cost of a final concrete tunnel lining even in good rock, it is common in Norway to leave shotcrete and rock bolts as the final protection (also in large sports halls). Some 160 km of our main road tunnels have S + B or S(fr) + B as the final liner, even in poor rock. A significant portion of these kilometres are in sub-sea tunnels, where corrosion has been shown not to be a problem when good quality concretes, *i.e.*, C45 or better, are used as the basis for shotcrete design. The corrosion of lattice girders and steel mesh due to shadow effects when spraying onto reinforcement are absent in steel fibre reinforced shotcrete, and the low permeabilities (10^{-13} to 10^{-14}m/s) and discontinuous nature of the fibres mean that galvanic action causing accelerated reinforcement corrosion is not experienced with S(fr).

For the above reasons NMT appears to be superior to NATM, which is the most publicised tunnelling philosophy for achieving moderately priced tunnels in soft ground conditions. The recent problems with NATM in London Clay at Heathrow airport may have been caused by the excessive rebound that is experienced with dry process shotcreting. Invert panels of poor quality shotcrete were being replaced when collapse of (eventually) three parallel excavations began. Use of S(fr), specifically wet process shotcrete, in place of dry process S(mr) where the mesh reinforcement prevents uniformity, may be the answer for improving NATM, if this method of tunnelling is resumed in London during 1995.

The main components of NMT are ***summarised*** in Figure 1 (top). In our conceptual NMT design desk, the upper three left-hand drawers form the usual basis for NMT design and application. In a large project, the two upper right-hand drawers, consisting of seismic measurements and numerical verification may also be utilised. The most cost-effective result for NMT will be achieved if the contract can be based on the flexible Norwegian Tunnel Contract System. Details of the potential contents of each NMT drawer are shown in Figure 1 (bottom). In this paper, we will be looking at some details of the upper four drawers.

INTRODUCTION TO THE Q-SYSTEM

Since bolting and shotcrete acts both as the primary (temporary) and secondary (final) lining in most tunnels in Norway, there is no possibility of relying on a subsequent concrete lining for covering poor workmanship or incorrect design concepts. Consequently, the design of the correct rock bolt spacing (and length) and the correct thickness of shotcrete (unreinforced or steel fibre reinforced) is unusually important.

NGI design of primary and secondary reinforcement for some 1,000 km of hydropower and main road tunnels during the last 20 years has been based exclusively on the Q-system of rock mass characterisation, which was developed from exhaustive case record synthesis in the early 1970s (Barton, Lien and Lunde, 1974). A good many of the case records were from Scandinavia, but since this time the Q-system has been used extensively in softer rocks in many parts of the world by a large number of consultants and contractors. On many projects it is used as a basis for defining support class for payment purposes.

The rock mass quality, which ranges over six orders of magnitude, is described by the six parameters given below:

$$Q = \frac{RQD}{J_n} \times \frac{J_r}{J_a} \times \frac{J_w}{SFR} \qquad (1)$$

where Q = quality number (0.001 for squeezing clay, 1000 for massive, unjointed rock)
RQD% = modified core recovery (counting only pieces $\geq$ 10 cm in length) (rating 10 to 100%)
J_n = joint set number (rating 0.5 to 20)
J_r = joint roughness number (rating 0.5 to 4)
J_a = joint alteration number (rating 0.75 to 20)
J_w = joint water reduction factor (rating 0.05 to 1.0)
SFR = stress reduction factor (rating 0.5 to 400)

The Q-value is given on the horizontal axis of the support design chart shown in Figure 2. The individual ratings are chosen from Table 1. A user-friendly reminder of these ratings is given in the histogram field logging chart shown in Figure 3.

The vertical axis of the support design chart shown in Figure 2 shows tunnel (or cavern) span width (or height) divided by a factor ESR which determines the desired level of safety. Table 2, which lists recommended values of ESR has the effect of providing heavier rock support for the most critical excavations (those with low ESR).

Table 1 Ratings for individual Q-parameters.

1. Rock Quality Designation		RQD
A	Very poor	0 - 25
B	Poor	25 - 50
C	Fair	50 - 75
D	Good	75 - 90
E	Excellent	90 - 100

Note: i) Where RQD is reported or measured as ≤ 10 (including 0), a nominal value of 10 is used to evaluate Q.
ii) RQD intervals of 5, *i.e.*, 100, 95, 90, *etc.*, are sufficiently accurate.

2. Joint Set Number		J_n
A	Massive, no or few joints	0.5 - 1.0
B	One joint set	2
C	One joint set plus random joints	3
D	Two joint sets	4
E	Two joint sets plus random joints	6
F	Three joint sets	9
G	Three joint sets plus random joints	12
H	Four or more joint sets, random, heavily jointed, *"sugar cube", etc.*	15
J	Crushed rock, earthlike	20

Note: i) For intersections, use (3.0 × J_n)
ii) For portals, use 2.0 × J_n)

3. Joint Roughness Number		J_r
a) Rock-wall contact, and b) rock-wall contact before 10 cm shear		
A	Discontinuous joints	4
B	Rough or irregular, undulating	3
C	Smooth, undulating	2
D	Slickensided, undulating	1.5
E	Rough or irregular, planar	1.5
F	Smooth, planar	1.0
G	Slickensided, planar	0.5

Note: i) Descriptions refer to small scale features and intermediate scale features, in that order.

c) No rock-wall contact when sheared		
H	Zone containing clay minerals thick enough to prevent rock-wall contact	1.0
J	Sandy, gravelly or crushed zone thick enough to prevent rock-wall contact	1.0

Note: i) Add 1.0 if the mean spacing of the relevant joint set is greater than 3m.
ii) J_r = 0.5 can be used for planar slickensided joints having lineations, provided the lineations are oriented for minimum strength.

4. Joint Alteration Number		ϕ_r approx.	J_a
a) Rock-wall contact (no mineral fillings, only coatings)			
A	Tightly healed, hard, non-softening, impermeable filling, *i.e.*, quartz or epidote		0.75
B	Unaltered joint walls, surface staining only	25-35°	1.0
C	Slightly altered joint walls. Non-softening mineral coatings, sandy particles, clay-free disintegrated rock, *etc.*	25-30°	2.0
D	Silty- or sandy-clay coatings, small clay fraction (non-softening)	20-25°	3.0
E	Softening or low friction clay mineral coatings, *i.e.*, kaolinite or mica. Also chlorite, talc, gypsum, graphite, *etc.*, and small quantities of swelling clays.	8-16°	4.0
b) Rock-wall contact before 10 cm shear (thin mineral fillings)			
F	Sandy particles, clay-free disintegrated rock, *etc.*	25-30°	4.0
G	Strongly over-consolidated non-softening clay mineral fillings (continuous, but <5mm thickness)	16-24°	6.0
H	Medium or low over-consolidation, softening, clay mineral fillings (continuous, but <5mm thickness)	12-16°	8.0
J	Swelling-clay fillings, *i.e.*, montmorillonite (continuous, but <5mm thickness). Value of J_a depends on percent of swelling clay-size particles, and access to water, *etc.*	8-12°	8-12
c) No rock-wall contact when sheared (thick mineral fillings)			
KLM	Zones or bands of disintegrated or crushed rock and clay (see G, H, J for description of clay condition)	6-24°	6, 8, or 8-12
N	Zones or bands of silty- or sandy-clay, small clay fraction (non-softening)	-	5.0
OPR	Thick, continuous zones or bands of clay (see G, H, J for description of clay condition)	6-24°	10, 13, or 13-20

5. Joint Water Reduction Factor		approx water pres. (kg/cm²)	J_w
A	Dry excavations or minor inflow, *i.e.*, <5 l/min locally	<1	1.0
B	Medium inflow or pressure, occasional outwash of joint fillings	1-2.5	0.66
C	Large inflow or high pressure in competent rock with unfilled joints	2.5-10	0.5
D	Large inflow or high pressure, considerable outwash of joint fillings	2.5-10	0.33
E	Exceptionally high inflow or water pressure at blasting, decaying with time	>10	0.2-0.1
F	Exceptionally high inflow or water pressure continuing without noticeable decay	>10	0.1-0.05

Note: i) Factors C to F are crude estimates. Increase J_w if drainage measures are installed.
ii) *Special problems caused by ice formation are not considered.*

6. Stress Reduction Factor				SRF
a) Weakness zones intersecting excavation, which may cause loosening of rock mass when tunnel is excavated				
A	Multiple occurrences of weakness zones containing *clay* or chemically disintegrated rock, very loose surrounding rock (any depth)			10
B	Single weakness zones containing *clay* or chemically disintegrated rock (depth of excavation ≤ 50m)			5
C	Single weakness zones containing *clay* or chemically disintegrated rock (depth of excavation > 50m)			2.5
D	Multiple shear zones in competent rock (*clay-free*), loose surrounding rock (any depth)			7.5
E	Single shear zones in competent rock (*clay-free*) (depth of excavation ≤ 50m)			5.0
F	Single shear zones in competent rock (*clay-free*) (depth of excavation > 50m)			2.5
G	Loose, open joints, heavily jointed or "sugar cube", *etc.* (any depth)			5.0

Note: i) Reduce these values of SRF by 25-50% if the relevant shear zones only influence but do not intersect the excavation.

b) Competent rock, rock stress problems		σ_c/σ_1	σ_θ/σ_c	SRF
H	Low stress, near surface, open joints	>200	<0.01	2.5
J	Medium stress, favourable stress condition	200-10	0.01-0.3	1
K	High stress, very tight structure. Usually favourable to stability, may be unfavourable for wall stability.	10-5	0.3-0.4	0.5-2
L	Moderate slabbing after >1 hour in *massive* rock	5-3	0.5-0.65	5-50
M	Slabbing and rock burst after a few minutes in *massive* rock	3-2	0.65-1	50-200
N	Heavy rock burst (strain-burst) and immediate dynamic deformations in *massive* rock	<2	>1	200-400

Note: ii) For strongly anisotropic virgin stress field (if measured): when $5 \le \sigma_1/\sigma_3 \le 10$, reduce σ_c to $0.75\sigma_c$. When $\sigma_1/\sigma_3 > 10$, reduce σ_c to $0.5\sigma_c$, where σ_c = unconfined compression strength, σ_1 and σ_3 are the major and minor principal stresses, and σ_θ = maximum tangential stress (estimated from elastic theory).
iii) Few case records available where depth of crown below surface is less than span width. Suggest SRF increase from 2.5 to 5 for such cases (see H).

c) Squeezing rock: plastic flow of incompetent rock under the influence of high rock pressure		σ_θ/σ_c	SRF
O	Mild squeezing rock pressure	1-5	5-10
P	Heavy squeezing rock pressure	>5	10-20

Note: iv) Cases of squeezing rock may occur for depth H > 350 $Q^{1/3}$ (Singh *et al.*, 1992). Rock mass compression strength can be estimated from q = 0.7 γ $Q^{1/3}$(MPa) where γ = rock density in kN/m³ (Singh, 1993).

d) Swelling rock: chemical swelling activity depending on presence of water		
R	Mild swelling rock pressure	5-10
S	Heavy swelling rock pressure	10-15

Note: J_r and J_a classification is applied to the joint set or discontinuity that is least favourable for stability both from the point of view of orientation and shear resistance, τ (where $\tau = \sigma_n \tan^{-1}(J_r/J_a)$). Choose the most likely feature to allow failure to initiate.

$$Q = \frac{RQD}{J_n} \times \frac{J_r}{J_a} \times \frac{J_w}{SRF}$$

Table 2 Summary of recommended ESR values (updated) for selecting safety level.

Type of Excavation		ESR
A	Temporary mine openings, *etc.*	*ca* 2-5
B	Permanent mine openings, water tunnels for hydropower (exclude high pressure penstocks), pilot tunnels, drifts and headings for large openings, surge chambers	1.6-2.0
C	Storage caverns, water treatment plants, minor road and railway tunnels, access tunnels	1.2-1.3
D	Power stations, major road and railway tunnels, civil defence chambers, portals, intersections	0.9-1.1
E	Underground nuclear power stations, railway stations, sports and public facilities, factories, major gas pipeline tunnels	0.5-0.8

It should be noted that Figure 2 and Table 1 represent recent improvements and updating of the Q-system support recommendations. Grimstad and Barton (1993)have reported on the inclusion of some 1,050 new case records from which the updated support chart is based. In particular, the extensive use of fibre reinforced shotcrete is incorporated in place of the earlier mesh reinforced variety S(mr), which has not been used in Norway during the past ten years. [Those projects which do not have access to S(fr) technology should utilise the original (1974) Q-system support recommendations which specifically address S(mr) + B support methods.]

Although the Q-system is used during field mapping for forecasting conditions, for estimating tunnel reinforcement needs, and for looking at costs and possible construction schedules, it is essentially a system to be used for design-as-you-drive. Figure 4 shows examples of tunnel mapping and reinforcement design for the case of a large 160m^2 hydropower tunnel (left) and for a TBM driven sewage tunnel (right). The two cases shown pre-date the shift to fibre reinforced shotcrete technology, and recommendations for mesh reinforced S(mr) and bolting are therefore shown.

UTILISATION OF SEISMIC MEASUREMENTS FOR TUNNEL FORECASTS

Recently, some promising new links have been established between seismic velocity and rock mass quality, such that the P-wave velocity (V_p) from remote sensing can be used in effect to estimate likely tunnel support requirements. Clearly this is not as straightforward as it sounds, because tunnel depth, rock porosity, water saturation and rock compressive strength all influence the

seismic velocity. The seismic refraction technique will also often lack the penetrative power needed to represent conditions at tunnel depth. This limitation has on occasion been bypassed in recent years by the use of cross-hole measurements and tomographic analysis. In this way, the quality of the recovered rock core (*i.e.*, that measured by RQD, joint frequency or Q-value) can be directly compared to the adjacent velocity tomograms. This calibration then allows rock quality to be predicted between the boreholes.

Two examples from Norwegian projects are illustrated in Figure 5. The upper diagram shows the principle of measurement with transmission from one borehole (using 1 gm detonators or piezoelectric sources) to a string of receivers (*i.e.*, hydrophones or 3D accelerometers) in the adjacent hole which may be 10, 50 or even 100 metres away. The measurements shown are from the Oslo Tunnel which was driven in good quality shale and limestone beneath soft clays. The lower tomogram is from the Olympic cavern site at Gjøvik, where pre-construction surveys in the well jointed gneiss helped to locate the cavern in rock of optimum quality.

Figure 6 shows a simplified relationship between V_p, Q, F and RQD. The fracture (or joint) frequency F (m^{-1}) and RQD (%) and their approximate relation to V_p (m/s) are based on work by Sjøgren *et al.* (1979). More than 100 km of seismic refraction surveys and nearly 3 km of drill core analysis in a variety of hard non-porous rocks form the basis for these relations.

The approximate relation between Q and V_p shown in Figure 6 is based on a variety of rock conditions in Norway, Hong Kong and China. In general the rocks, even if crushed and clay bearing, have been of the ***non-porous*** variety (*i.e.*, excluding chalk and porous sandstones) and the measurements have been in the 20 to 40m range of depths. As will be noted from Table 3, the basic relation between Q and V_p is very simple and easy to recall:

Table 3 Simplified relation between Q and V_p.

Q	0.01	0.1	1.0	10	100	1000
V_p km/s	1.5	2.5	3.5	4.5	5.5	6.5

$$V_p \approx \log Q + 3.5 \quad \text{km/s} \qquad (2)$$

Recent analysis of a wider range of rock conditions encompassing depths up to 1,000m, rock matrix porosities up to 30% and laboratory uniaxial compression strengths from about 3 MPa to 200 MPa has resulted in the comprehensive ***rock quality chart*** shown in Figure 7. Besides the six Q-system parameters, this chart incorporates (in an approximate manner) the variables of depth, porosity and uniaxial strength , and also provides an estimate of the likely range of deformation moduli (for use in numerical analyses). It will be noted that the Q-value has been modified to the form:

$$Q_c = (Q)\frac{\sigma_c}{100} \quad (3)$$

In other words, when the uniaxial compression strength (σ_c) is more than 100 MPa, $Q_c > Q$, and when $\sigma_c < 100$ MPa, $Q_c < Q$. A Q-value of 10 for a hard rock site might have $Q_c = 20$ (when $\sigma_c = 200$ MPa), while a soft rock site with $Q = 10$ might have $Q_c = 0.5$ (when $\sigma_c = 5$ MPa). If the soft rock was overstressed by the planned depth of tunnel, it would of course probably have a Q-value much lower than 10 due to unfavourable σ_θ/σ_c ratios and increased SRF values. (See Table 1, part 6c and 6b.)

Example Heavily fractured chalk $Q = 1.0$
porosity = 10% $\sigma_c = 10$ MPa
$Q_c = 0.1$ $\therefore V_p$ at 50m depth $\approx$ 2.1 km/s
$\therefore V_p$ at 100m depth $\approx$ 2.5 km/s

In other words, measurement of a velocity of 2.1 km/s at 50m depth, with additional estimation of porosity (*i.e.*, 10%) would place one at $Q_c \approx 0.1$ on the ***rock quality chart***. Consequently, following equation 3, one could deduce a Q-value as low as 1.0 if it was known from experience that the uniaxial strength of the chalk was about 10 MPa. Reference to Figure 2 would show that a 10m span tunnel (at this 50m depth in the chalk) would need the following final rock support:

S(fr) 9 cm
B 1.7m c/c, length 3.0m

For numerical analysis of the same tunnel, a mean deformation modulus for the rock mass of about 3 GPa would be used, with a worst case value of 0.5 GPa.

The equations quoted in Figure 7 for the central trend line (filled circles):

$$V_p \approx \log Q + 3.5 \quad (4)$$

$$\overline{M} \approx 10 \times Q^{\left(\frac{1}{3}\right)} \quad (5)$$

$$\overline{M} \approx 10 \times 10^{\left(\frac{V_p - 3.5}{3}\right)} \quad (6)$$

have been shown to give a better fit for a wider range of rock types when Q is replaced by Q_c. The further adjustment for depth (increasing velocity) and for porosity (reducing velocity) are made by suitable addition and subtraction (of velocity) within the sloping lines in Figure 7.

DESCRIPTION OF JOINTING FOR NUMERICAL MODELLING

Tunnelling design in jointed rock masses has been shown in the foregoing sections to be amenable to empirical methods of analysis, through rock mass classification of the degree of jointing and its character, *i.e.*, rough, smooth, clay filled, *etc.* In certain cases where conditions are critical or where unusual excavation shapes or span widths are to be designed it is helpful to be able to supplement the empirical design with numerical analyses as a quality control of the empirical designs.

Although in the past much use has been made of linear elastic assumptions in finite element analyses of rock mass behaviour, it is now known that such optimism is misplaced unless excavations are quite small and are undertaken with minimal disturbance and in quite massive rock. Larger excavations in "normal" jointed rock, whether this is weak or hard rock, tend to result in non-linear behaviour, with opening and shearing of joints close to the opening such that the effective deformation modulus (and seismic velocity) may be much reduced close to the opening, and possible increased a little further out in the rock mass where the main "load bearing ring" is established. An example of this is shown in Figure 8.

Since it is extremely difficult to choose appropriate reductions or increases of moduli for continued use of FEM type elastic models, the alternative approach is discrete modelling of the jointing, such that the stress changes caused by excavation are allowed to influence the jointing in a "natural" manner such that deformations and stress redistribution are modelled more realistically.

Figure 9 indicates diagrammatically some of the ways in which differently jointed rock masses respond to loading (which may in effect be caused by unloading in a perpendicular direction). The largely non-linear and hysteretic behaviour is caused by the interactions of stiffening behaviour of joints under closure (N) and by the softening behaviour under shear (S). Constitutive models of closure and shear behaviour for joints have been developed by Bandis *et al.* (1981) and Barton *et al.* (1985), using as input parameters easily obtainable parameters that describe the joint roughness (JRC) and the joint wall compression strength (JCS). The basic shear strength equation using these parameters is shown in Figure 10. It is seen to be a special case of the Mohr-Coulomb and Patton equations, taking account of variable roughness and variable rock compression strength.

$$\tau = \sigma_n \tan\left(\mathrm{JRC} \log \frac{\mathrm{JCS}}{\sigma_n} + \phi_r\right) \qquad (7)$$

In addition to the self weight tilt tests shown in Figure 11, all that is needed is a Schmidt rebound hammer for determining the input parameters JRC and JCS. Details are given by Barton and Bandis (1990). The typical range of JRC and JCS values for laboratory size joint samples in a variety of rocks are shown in

the histograms in Figure 12. The peak shear strength envelopes that fit the direct shear test data shown in the same figure are specifically for laboratory size (10 cm long) samples. Reduction factors for JRC and JCS are used for larger block sizes. These same formulations can of course be used for slope stability analyses for jointed rock, or for the tunnel models described below.

VERIFICATION OF EMPRICAL Q-DESIGN BY NUMERICAL UDEC-BB MODELS

The distinct element code called UDEC that was developed by Cundall (1980) for modelling jointed rock in two dimensions, has a subroutine termed "BB" for describing the non-linear behaviour of joints as briefly described above.

To demonstrate the capabilities of the code, the example of twin motorway tunnels of 16m span in granite is given in Figure 13. The input data for the two sets of joints and for the intact rock were obtained from inspection of core boxes and from field logging of joint characteristics. These jointed models of granite were first loaded in the unexcavated state with suitable vertical and horizontal effective stress levels. The tunnels were excavated to half span, numerically bolted, then excavated to full span and bolted again. The peak (maximum) responses to excavation once equilibrium was reached were as follows:

maximum stress	=	8.04 MPa
maximum displacement	=	3.9mm
maximum joint shearing	=	2.5mm
maximum bolt force	=	6.9 tons

The bolt forces are plotted at each location where bolts cross the modelled joints. If over-loading is evident in certain parts of the profile due to anisotropic loading, then the capacity of the bolts can be upgraded, *i.e.*, 25mm to 32mm ∅.

The modelled displacements appear reasonable with respect to the known rock mass quality ($Q_{mean} \approx 4.5$) and span width of 16m. Results can be checked against case records of tunnel and cavern deformations, using the normalised Q/SPAN plot shown in Figure 14. The value of Q/SPAN of 4.5/16 (=0.28) would suggest a typical 4mm of deformation (line BB) but with room for wide variation locally, *i.e.*, 2 to 10mm. This is in fact almost exactly what has been measured during recent construction of the tunnels in South East Asia.

THREE-DIMENSIONAL MODELLING

The development of the three-dimensional code 3DEC by Cundall and Itasca Inc. in the late 1980s (Cundall, 1988; Hart *et al.*, 1988) has advanced our ability to analyse excavation in jointed rock a significant stage further than that represented by UDEC. The tunnel and block structure shown in Figure 15

illustrates the power of three-dimensional visualisation of 3D joint structures. "Pilot tunnels" can be driven in different orientations to "investigate" the rock mass with "walk-in" representation of jointing in the roof or walls of a planned excavation. Subsequent application of internal and external boundary conditions and excavation stage-by-stage under stress gives the maximum possible information of mechanical response for important excavations. Systematic bolting can be applied as in UDEC.

CONCLUSIONS

1) Key aspects of the Norwegian Method of Tunnelling (NMT) have been described. These include use of a quantitative method of rock mass classification and use of fibre reinforced shotcrete and rock bolting as final support. This empirical design method is based on some 1,250 case records. Methods of recording the rock quality data during field mapping and for updating this during tunnel excavation have been illustrated.

2) Recent work showing a link between the rock mass Q-value and the seismic velocity V_p indicate considerable promise for predicting tunnel support needs from remote sensing. It is shown how V_p, Q and the deformation modulus (M) for the rock mass are interrelated, and roughly speaking how V_p and M may be influenced by the porosity of the rock, by the rock's compression strength and by the depth of the tunnel.

3) Methods of describing the non-linear strength and deformability behaviour of joints for use in distinct element numerical models such as UDEC have been outlined. It has been shown how the numerically predicted deformation magnitudes can be checked for reasonableness against case records of recorded deformations in tunnels and caverns using the normalising Q/SPAN term.

REFERENCES

Bandis, S., A. Lumsden and N. Barton, 1981, "Experimental studies of scale effects on the shear behaviour of rock joints", Int. J. of Rock Mech. Min. Sci. and Geomech. Abstr. 18, pp. 1-21.

Barton, N., R. Lien and J. Lunde, 1974, "Engineering classification of rockmasses for the design of tunnel support", Rock Mechanics, Vol. 6, No. 4, pp. 189-236.

Barton, N., S. Bandis and K. Bakhtar, 1985, "Strength, Deformation and Conductivity Coupling of Rock Joints", Int. J. Rock Mech. & Min. Sci. & Geomech. Abstr. Vol. 22, No. 3, pp. 121-140.

Barton, N. and S.C. Bandis, 1990, "Review of predictive capabilities of JRC-JCS model in engineering practice", International Symposium on Rock Joints. Loen 1990. Proceedings, pp. 603-610, 1990.

Cundall, P., 1980, "A generalized distinct element program for modelling jointed rock." Report PCAR-1-80, Contract DAJA37-79-C-0548, European Research Office, US Army. Peter Cundall Associates.

Cundall, P.A., 1988, "Formation of a Three-Dimensional Distinct Element Model - Part I: A Scheme to Detect and Represent Contacts in a System Composed of Many Polyhedral Blocks.", Int. J. Rock Mech. Min. Sci. & Geomech. Abstr., 25, pp. 107-116.

Grimstad, E. and N. Barton, 1993, "Updating of the Q-System for NMT", Proceedings of the International Symposium on Sprayed Concrete - Modern Use of Wet Mix Sprayed Concrete for Underground Support, Fagernes, 1993, (Eds Kompen, Opsahl and Berg. Norwegian Concrete Association, Oslo.

Hart, R., P. Cundall and J. Lemos, 1988, "Formation of a Three-Dimensional Distinct Element Model - Part II: Mechanical Calculaton for Motion and Interaction of a System Composed of Many Polyhedral Blocks." Int. J. Rock Mech. Min. Sci. & Geomech. Abstr., 25, pp. 117-126.

Kujundzic, B., Jovanovic, L. and Radosavljevic, Z., 1970: "A Pressure Tunnel Lining Using High-Pressure Grouting" (in French). Proc. 2nd Congress International Society for Rock Mechanics, Belgrade, Vol. 2, pp. 867-881.

Plichon, J.N., 1980, "Measurements of the thickness of the decompressed zone in an excavation under high overburden cover" in Analysis of Tunnel Stability by the Converence-Confinement Method, Underground space, 4, vol. 6 pp. 361-402.

Sjögren B., Øvsthus A. and Sandberg J., 1979, "Seismic classification of rock mass qualities". Geophysical Prospecting, Vol. 27, No. 2, pp. 409 - 442.

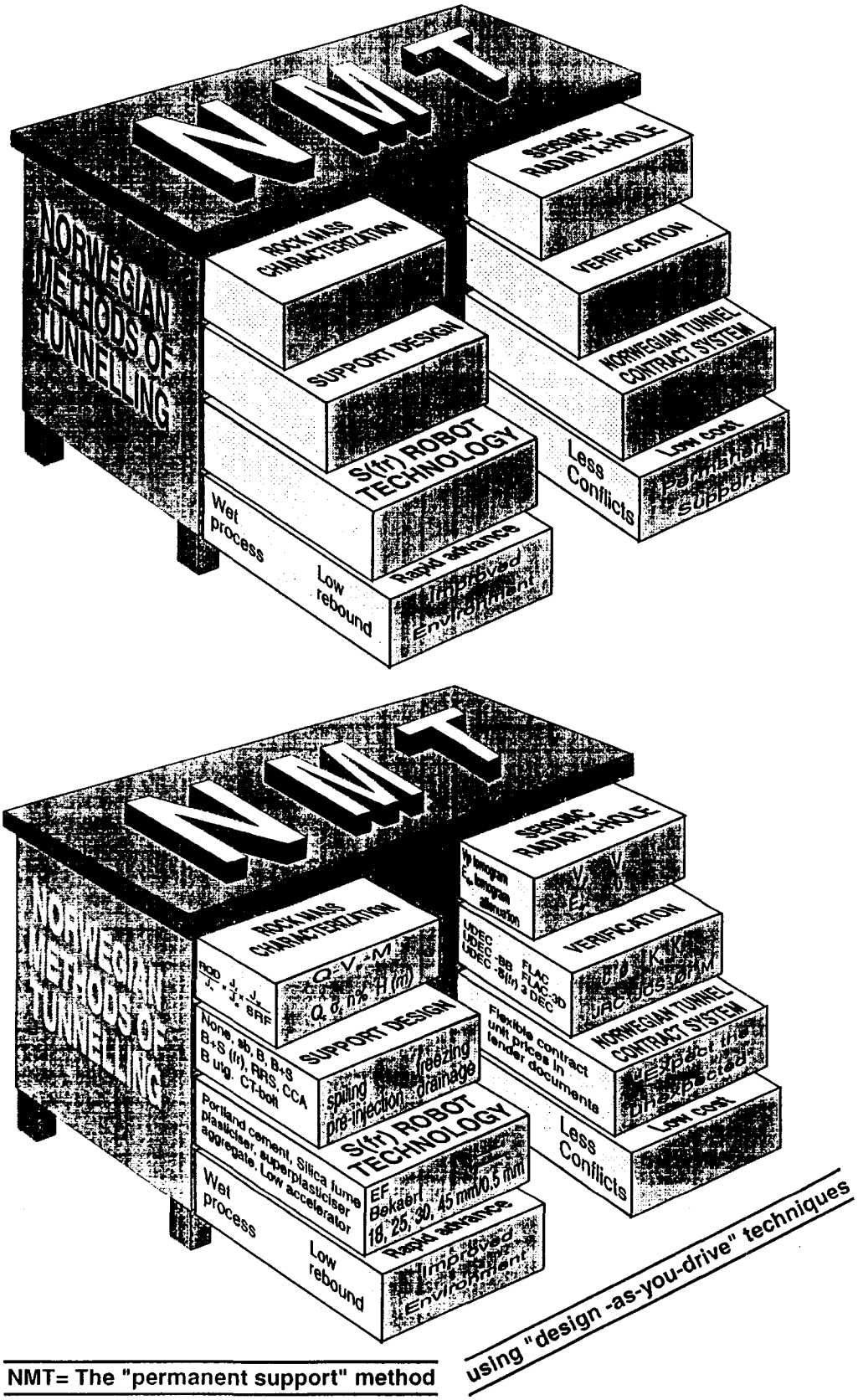

Figure 1 NMT design and execution.

PCo\Barton\articles\Korea-95.NMT

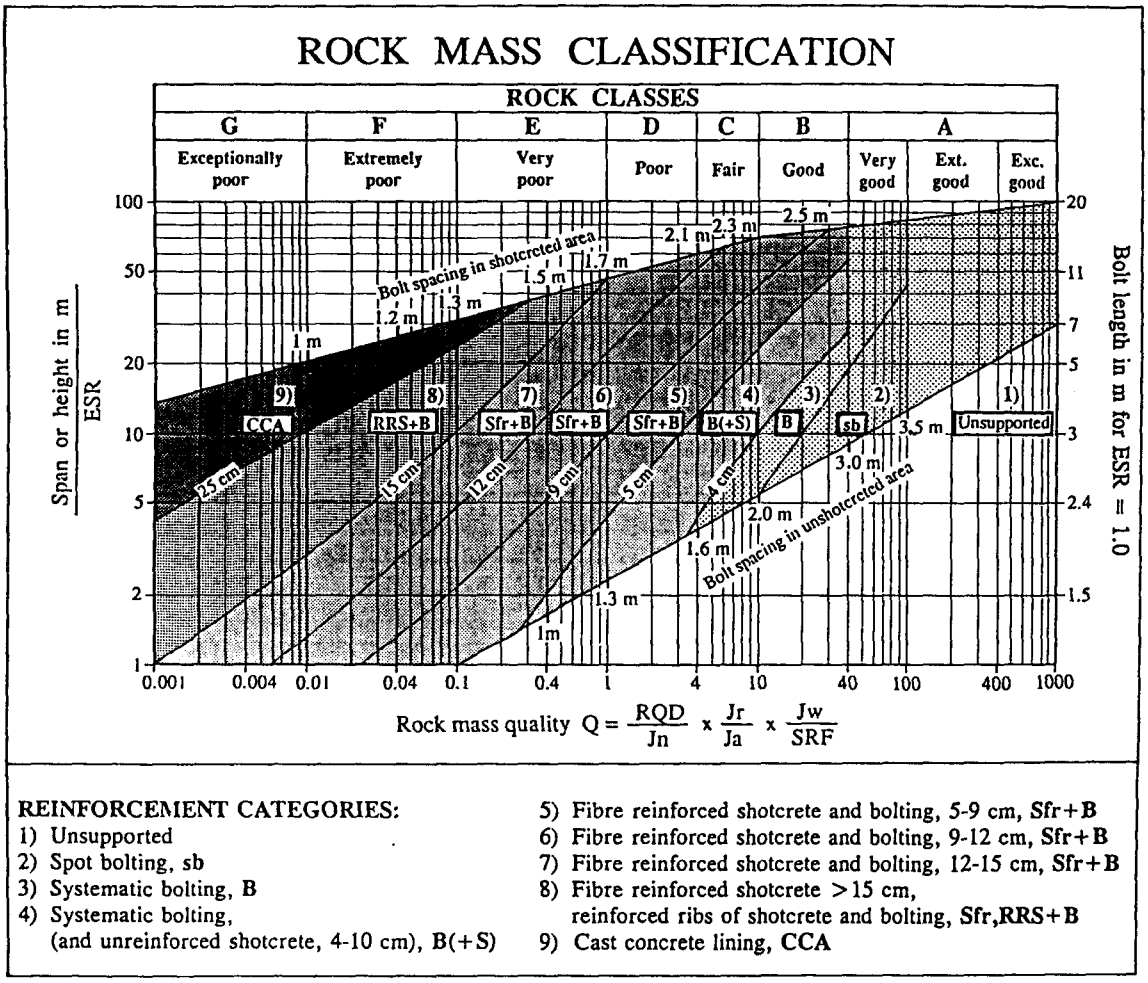

REINFORCEMENT CATEGORIES:

1) Unsupported
2) Spot bolting, sb
3) Systematic bolting, B
4) Systematic bolting, (and unreinforced shotcrete, 4-10 cm), B(+S)
5) Fibre reinforced shotcrete and bolting, 5-9 cm, Sfr+B
6) Fibre reinforced shotcrete and bolting, 9-12 cm, Sfr+B
7) Fibre reinforced shotcrete and bolting, 12-15 cm, Sfr+B
8) Fibre reinforced shotcrete >15 cm, reinforced ribs of shotcrete and bolting, Sfr,RRS+B
9) Cast concrete lining, CCA

Figure 2 The Q-system tunnel reinforcement design chart (Grimstad and Barton, 1993).

PCo\Barton\articles\Korea-95.NMT

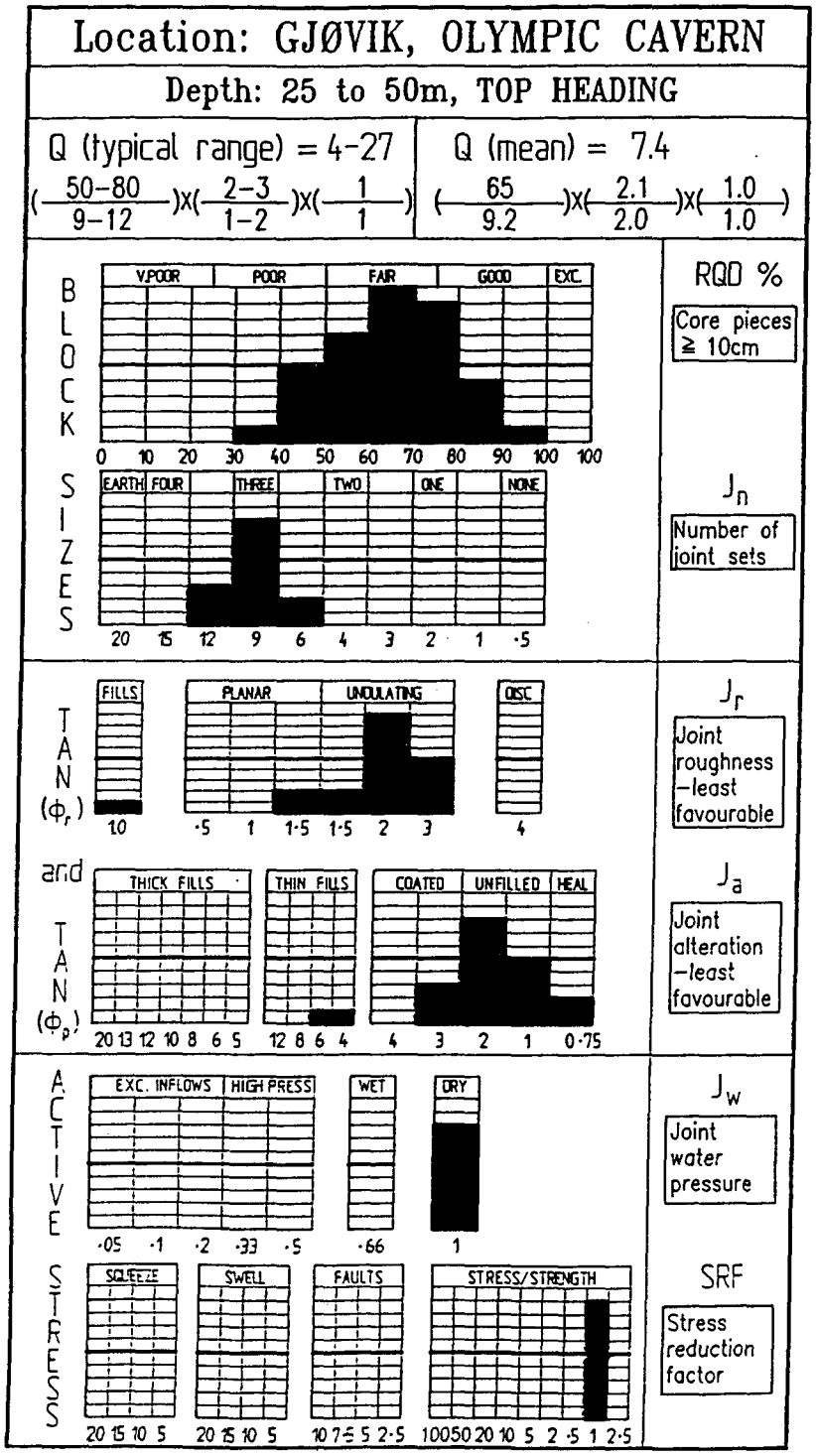

Figure 3 Logging chart for assembling Q-parameter statistics.

PCo\Barton\articles\Korea-95.NMT

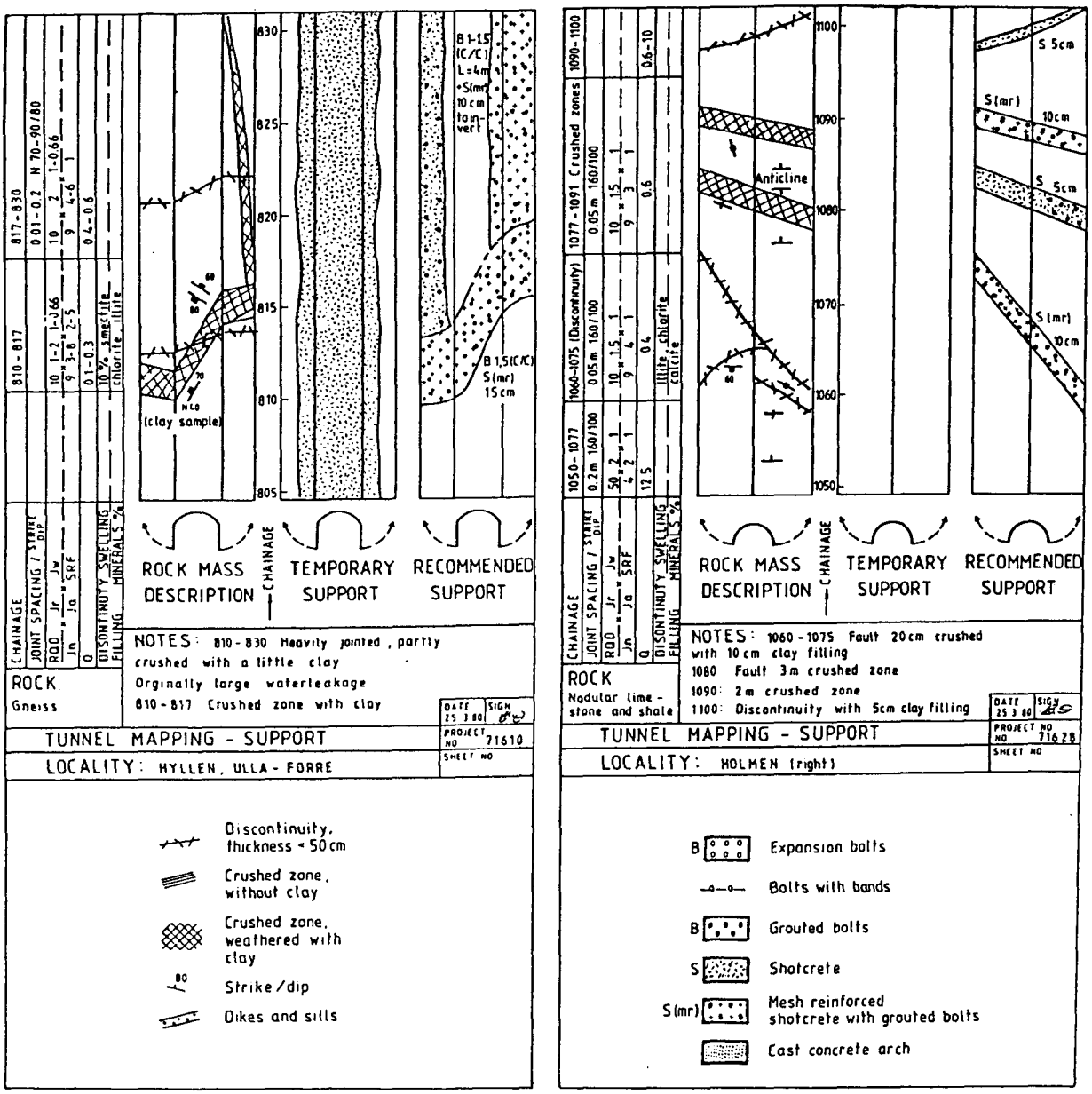

Figure 4 Tunnel mapping chart for design-as-you-drive decisions.

PCo\Barton\articles\Korea-95.NMT

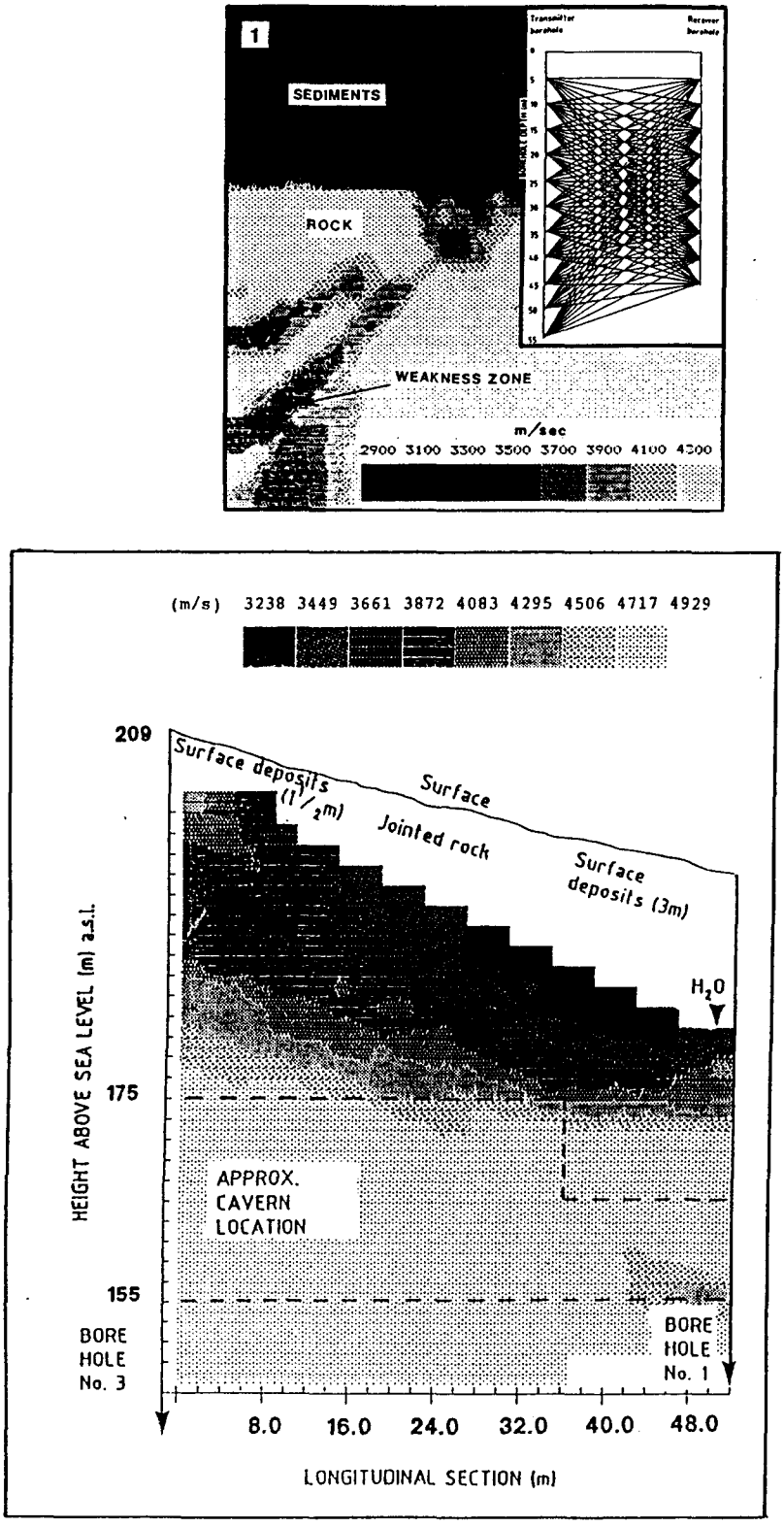

Figure 5 Seismic tomography showing measurement principle and typical results.

PCo\Barton\articles\Korea-95.NMT

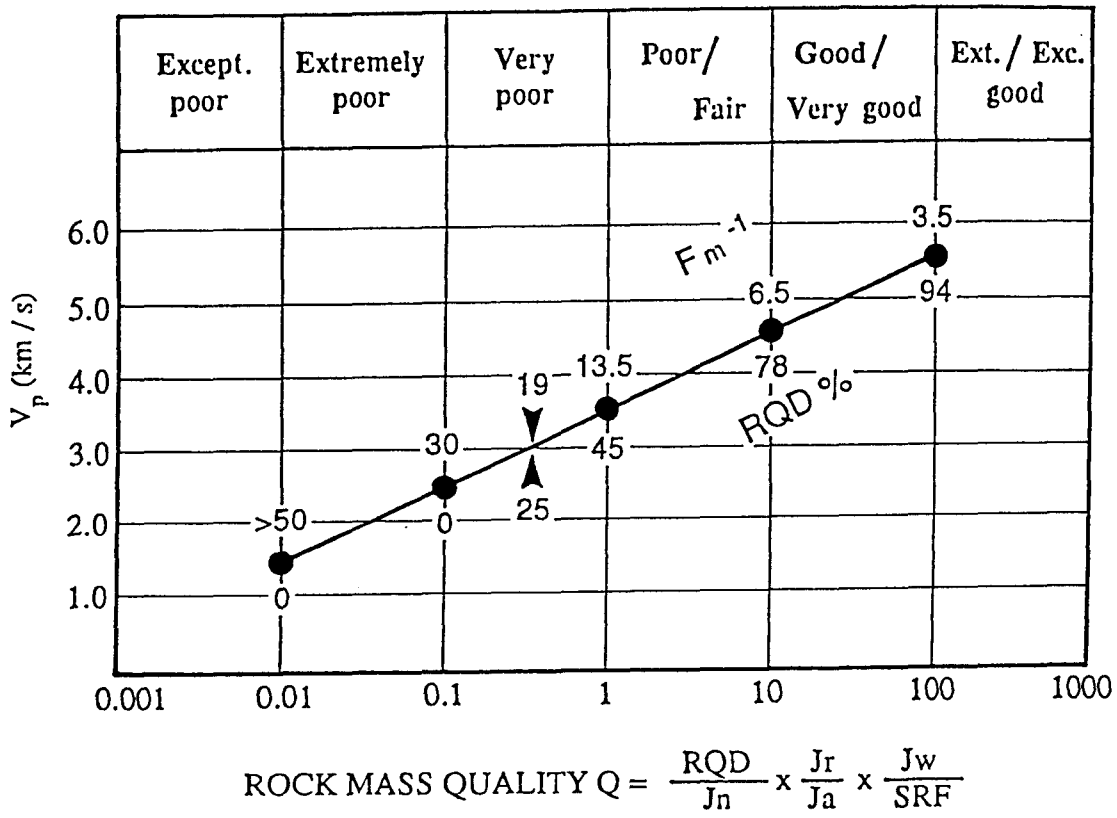

Figure 6 Simplified links between rock quality and seismic velocity.

PCo\Barton\articles\Korea-95.NMT

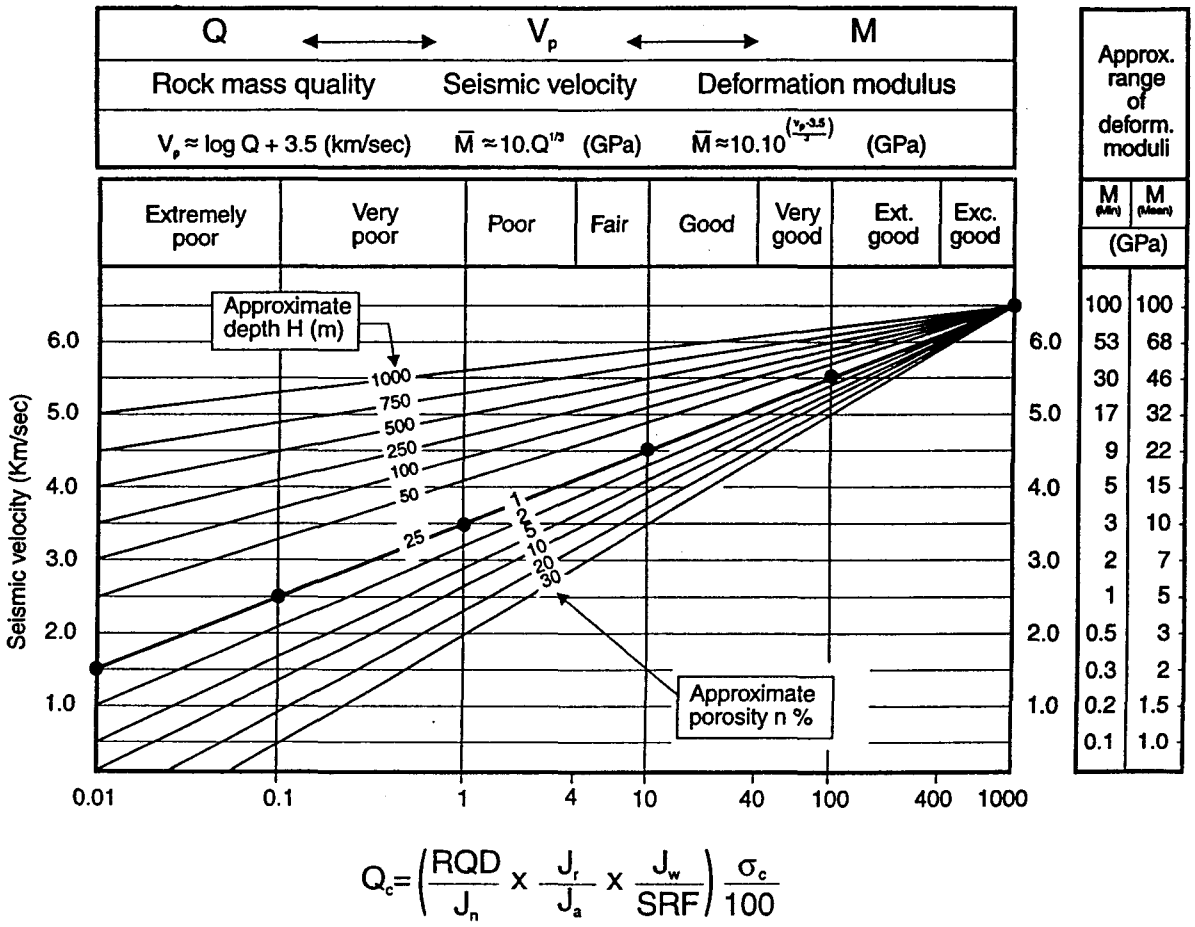

Figure 7 Rock mass quality chart for estimating the Q-value from seismic measurements

PCo\Barton\articles\Korea-95.NMT

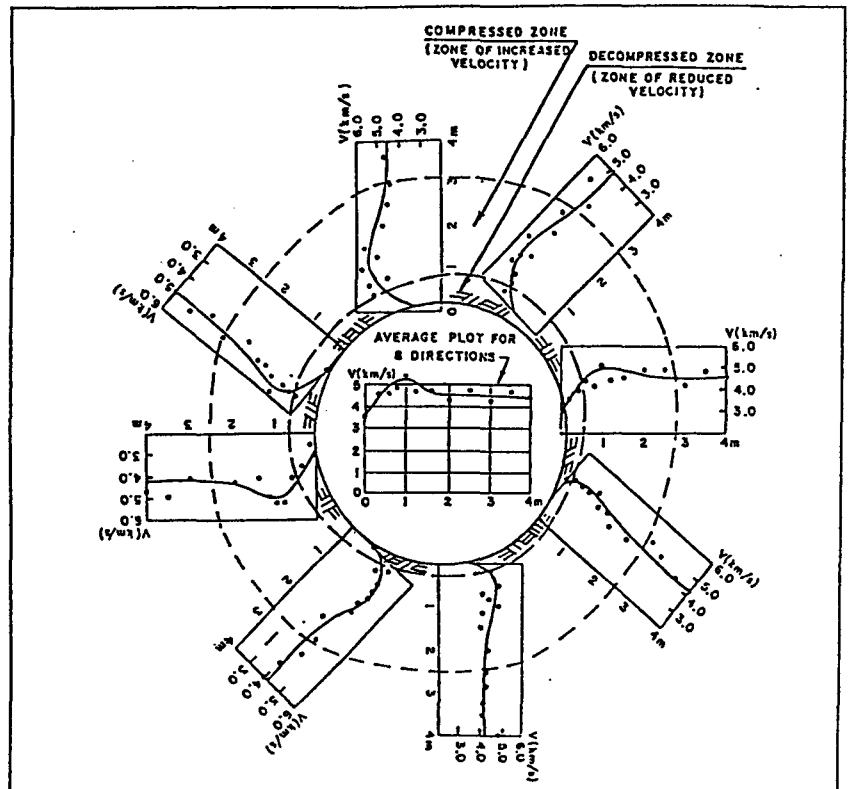

V = Longitudinal seismic velocity measured parallel to tunnel axis by cross hole measurement between two sets of 8 radial boreholes, 1.2m apart.

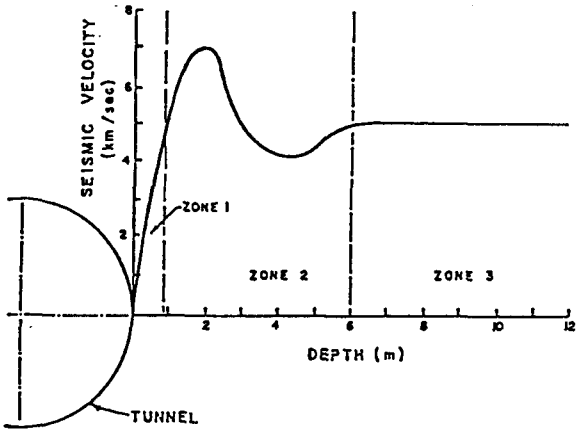

Zone 1 - Decompressed area near tunnel wall
Zone 2 - Intermediate area affected by tunnel construction
Zone 3 - Unaffected rock mass

Figure 8 Seismic measurements in circular tunnels showing effects of stress concentration on seismic velocity. (Kujundzic et al., 1970; and Plinchon, 1980)

PCo\Barton\articles\Korea-95.NMT

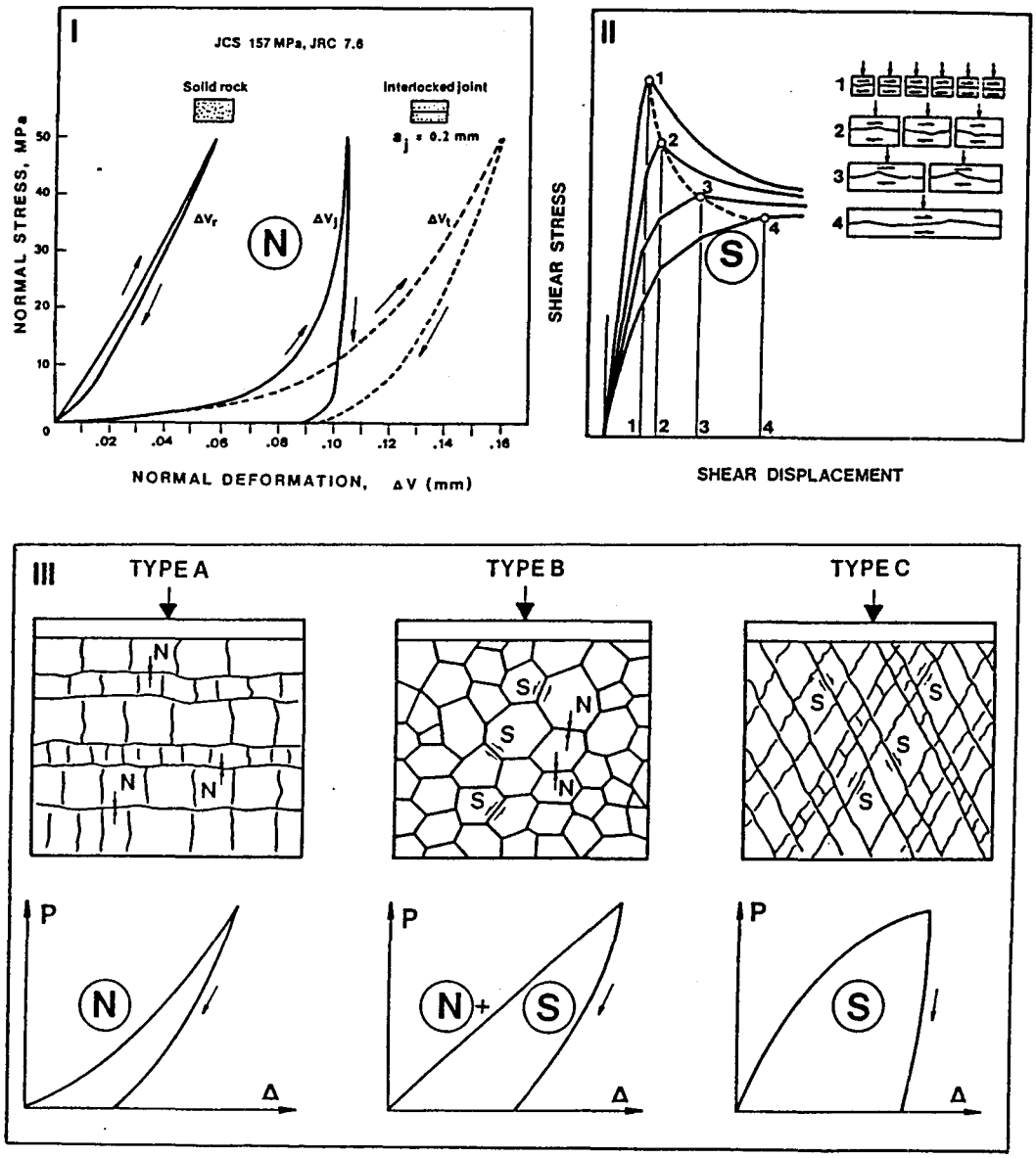

Figure 9 Some fundamental responses of jointed rock that have to be modelled numerically.

PCo\Barton\articles\Korea-95.NMT

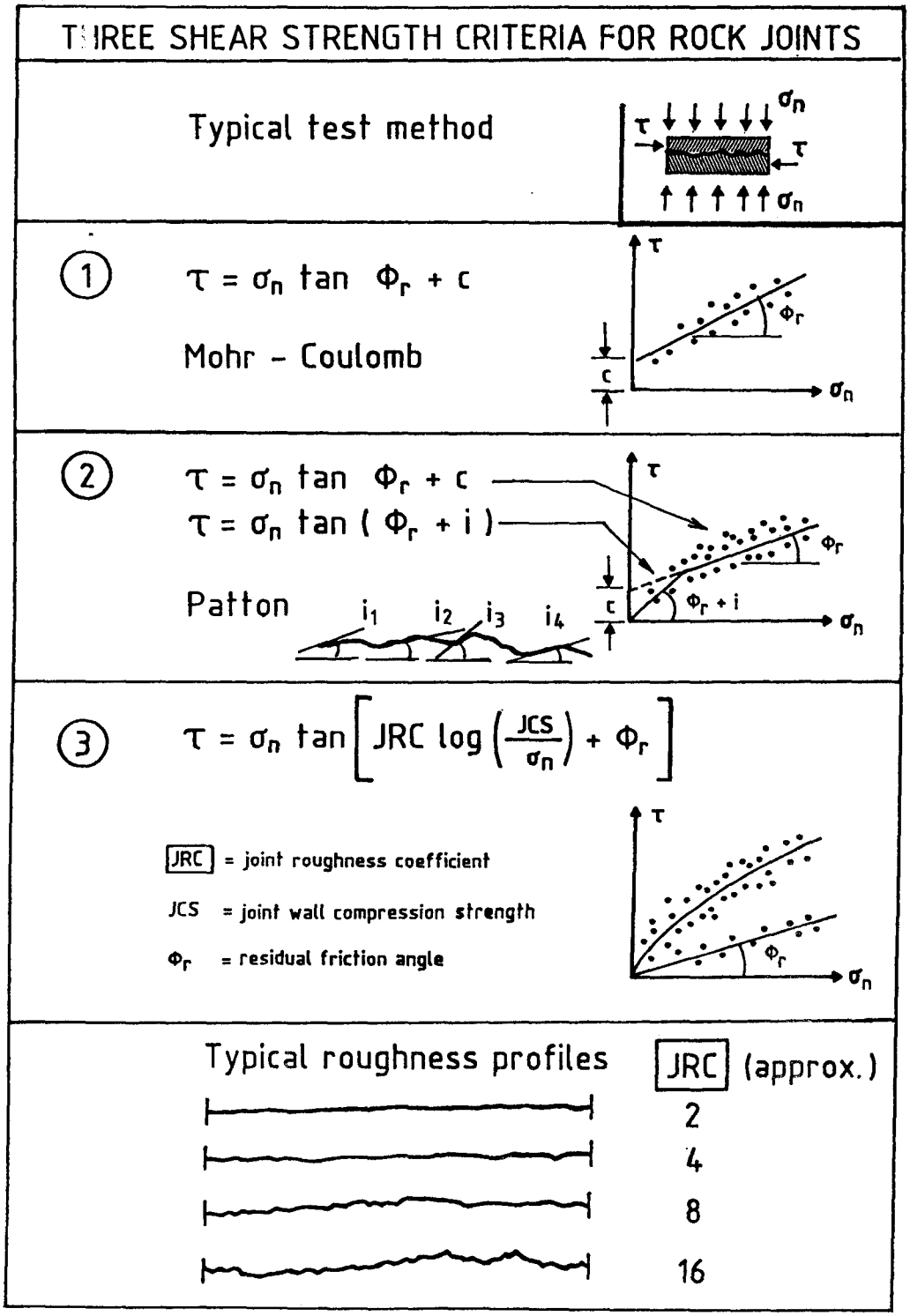

Figure 10 Modelling the shear behaviour of joints.

PCo\Barton\articles\Korea-95.NMT

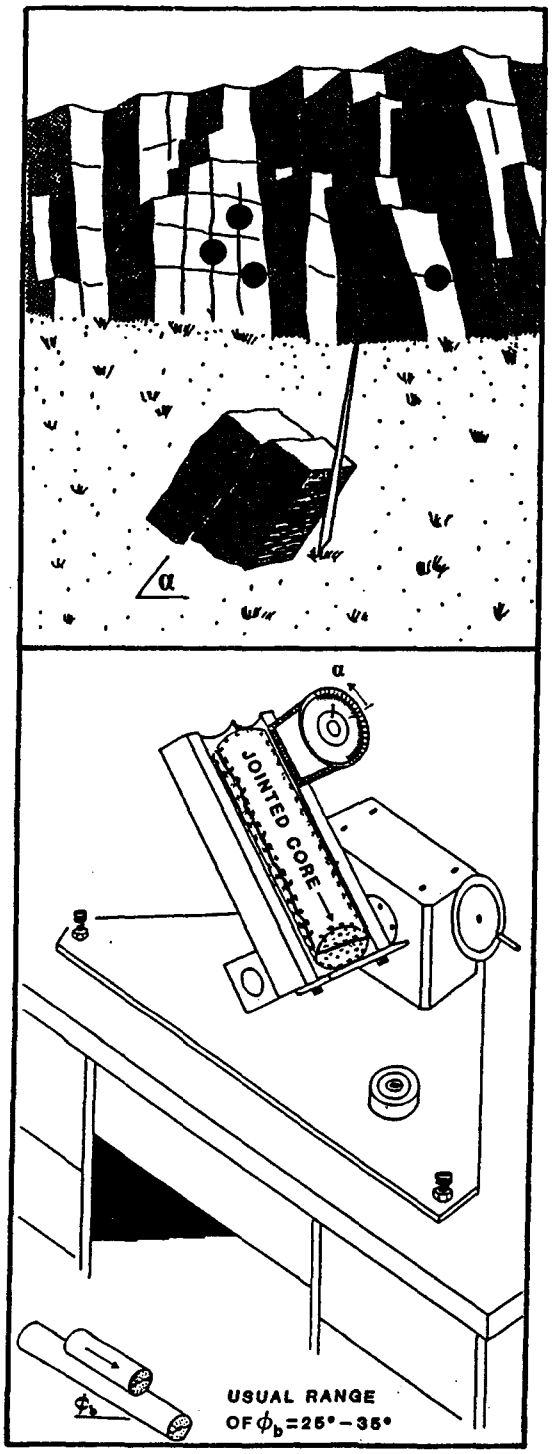

Figure 11 Self weight sliding or tilt tests for determining the joint roughness (JRC) of a joint.

PCo\Barton\articles\Korea-95.NMT

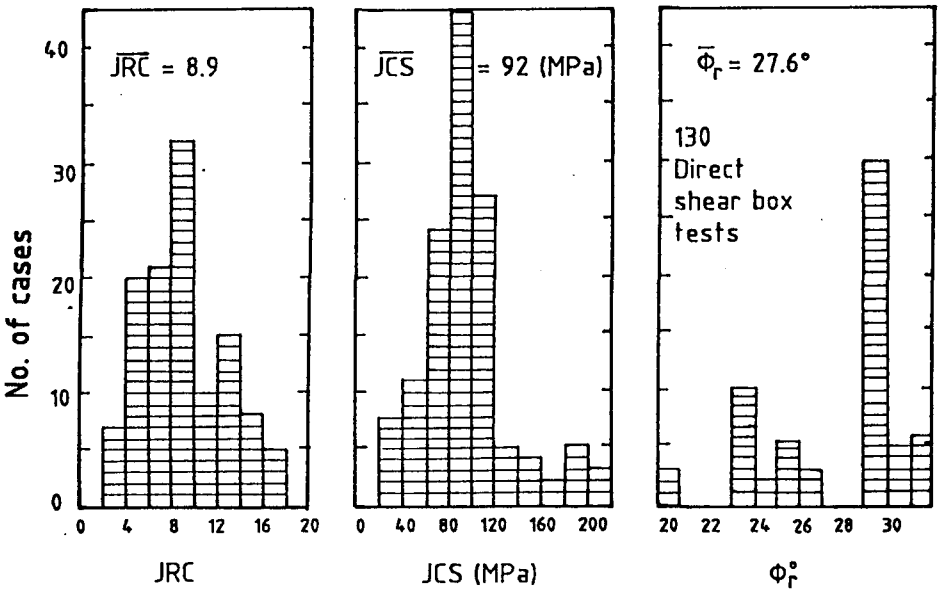

$$\Phi_{peak} = \Phi_r + i = \Phi_r + JRC \log_{10} (JCS/\sigma_n')$$

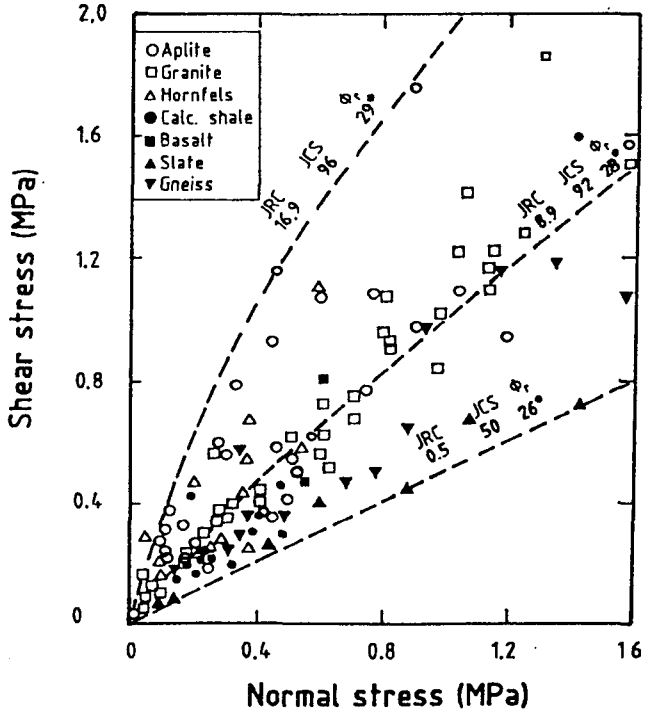

Figure 12 Typical values of JRC, JCS and ϕ_r from laboratory shear box tests of 130 joint samples.

PCo\Barton\articles\Korea-95.NMT

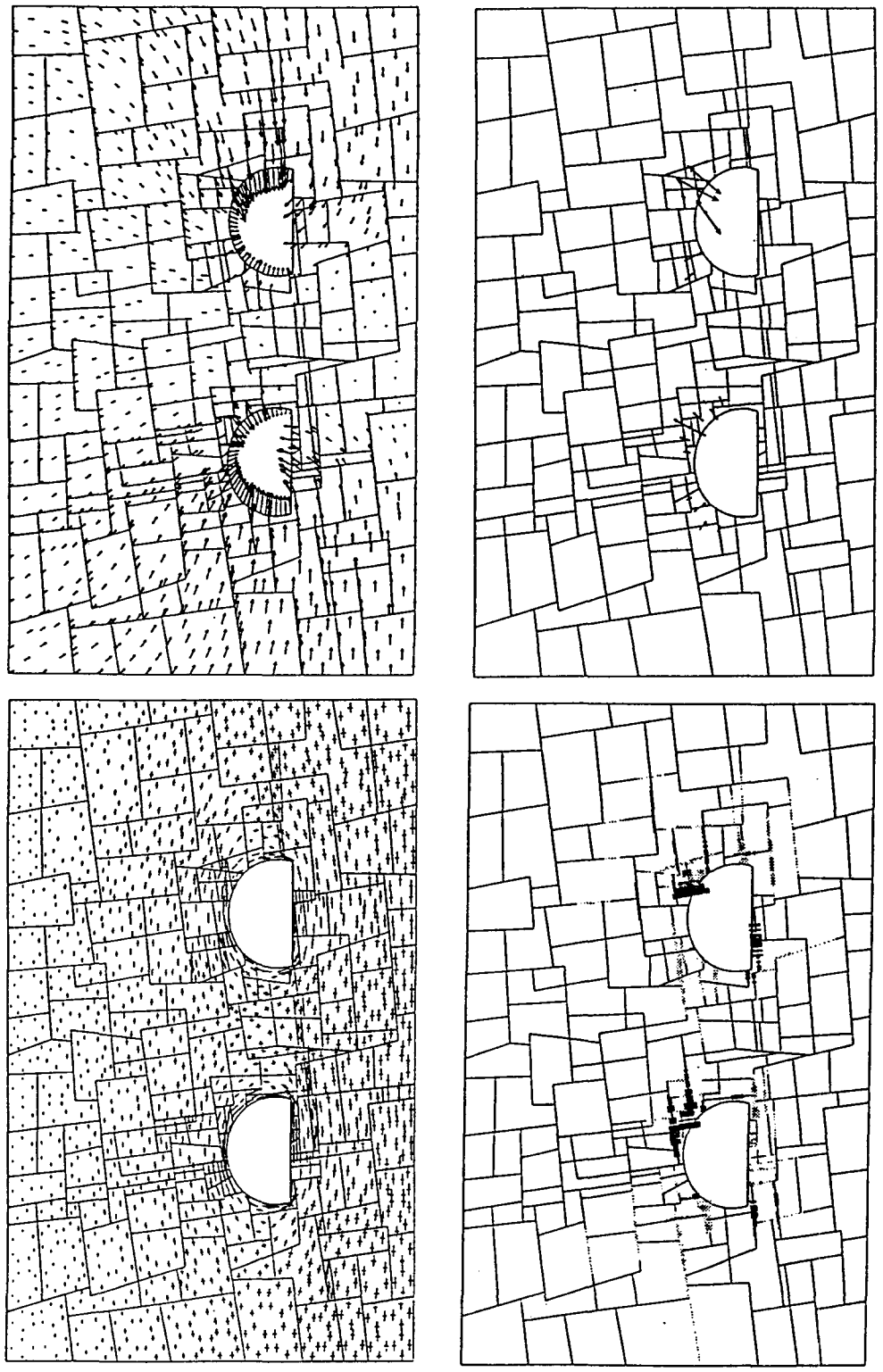

Figure 13 Examples of stress, deformation, joint shearing and bolt loading in a UDEC-BB model of tunnels in granite. (L. Backer, NGI report, 1993)

PCo\Barton\articles\Korea-95.NMT

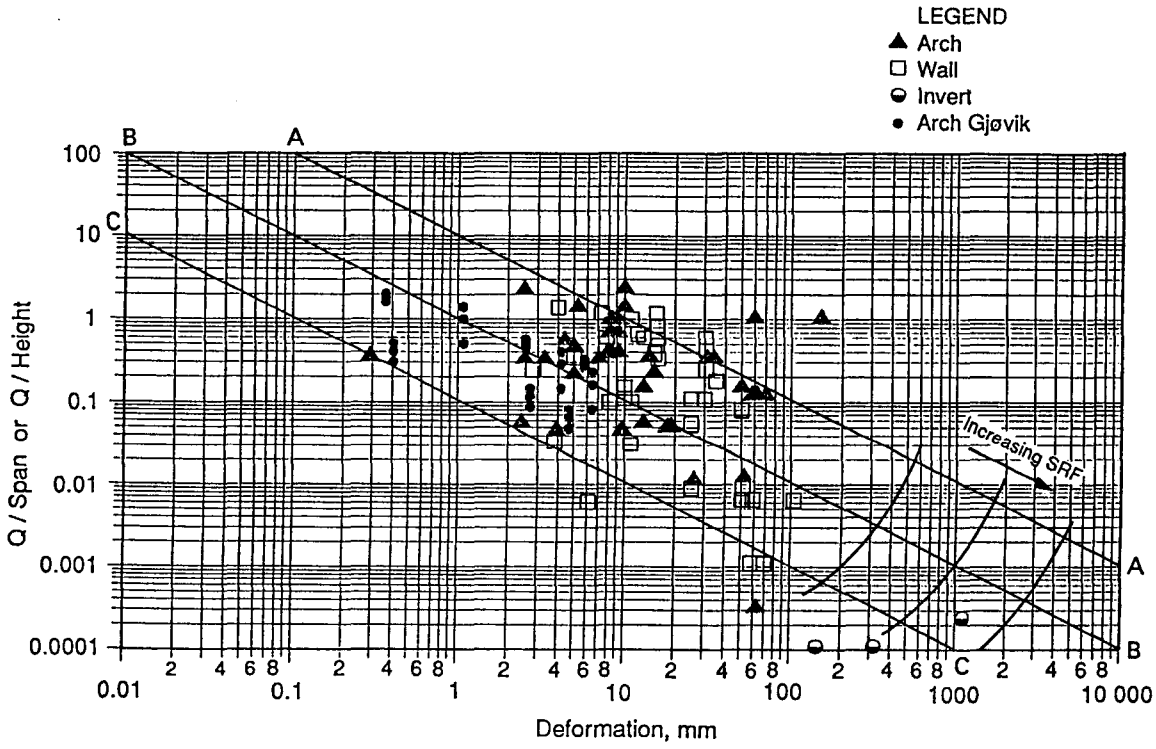

Figure 14 Measured deformations in tunnels and caverns as function of Q-value and dimension.

PCo\Barton\articles\Korea-95.NMT

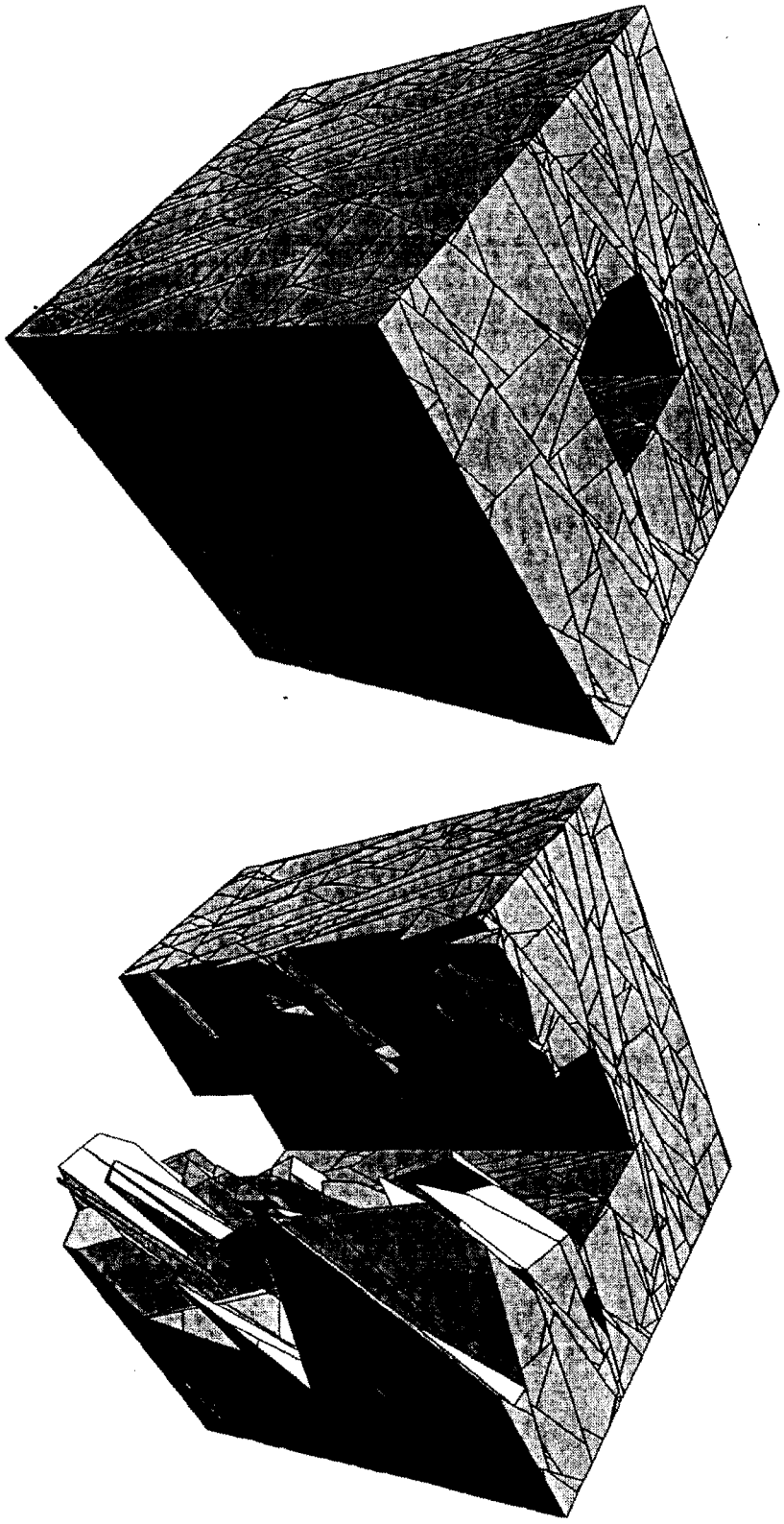

Figure 15 Three predominant joint sets and visualisation of this jointing within a tunnel.